Hysteresis Stress, Strain and Penetration Analysis of Spur Gear Assembly for Various Sustainable Design

Bharat Singh[1], *Shaymaa* Ahmed[2], *J* Sridevi[3], *B* Rajalakshmi[4*], *H* Pal Thethi[5], *Abhishek* Kaushik[6], *Vemuri Venkata Phani* Babu[7]

[1]Department of Mechanical Engineering, GLA University, Mathura, India-281406
[2]Hilla University College, Babylon, Iraq.
[3]Department of EEE, GRIET, Bachupally, Hyderabad, Telangana, India.
[4]Department of Computer Science, New Horizon College of Engineering, Bangalore, Karnataka, India.
[5]Lovely Professional University, Phagwara, India.
[6]Lloyd Institute of Engineering & Technology, Knowledge Park II, Greater Noida, Uttar Pradesh, India.
[7]Department of Mechanical Engineering, MLR Institute of Technology, Hyderabad, Telangana, India.

Abstract. This paper considers and compares the hysteresis stress and strain and the penetration property of spur gear assemblies based on three unique designs. Spur gear plays an important part in mechanical structures, and any mechanical setup should consider the execution of such a mechanical component under distinct designs to improve its mechanical productivity and sustainability. To explore the ways in which the mechanical behaviour of the designs varies with the design configurations, we integrate simulation analysis with an experimental study. The outcomes of this paper indicate considerable differences in both hysteresis stress, strain distribution, and penetration behavior measurements between three designs. The paper explains the stated disparities by the unique geometric layouts and material characteristics of each design. Furthermore, it emphasizes that some of the examined designs have lower hysteresis losses and favourable stress and strain distributions, which positively affects the long-term performance of gear systems. Other designs, however, exhibit severe penetration and stress concentrations leading to rapid gear wear and likely premature failure. In distinguishing these events, the present study offers a valuable approach to the parameters that influence the performance of gear systems and aids in the improvement of the design methodology.

Keyword-: Spur Gear Assembly, Hysteresis Stress, Hysteresis Strain, Penetration, Sustainability, Gear Systems.

* Corresponding Author : dr_rajalakshmi_inprint@yahoo.com.

1 Introduction

Hysteresis is one of the most salient features that influence the gears in a system where stress and strain of a material are dependent on its load-bearing capacity [1]. Gear systems work cyclically and this makes them prone to wear and tear. This has happened because, in each cycle there is a position or condition of the gear that changes and this results in fatigue failure [2]. This could be clarified by understanding that teeth penetration is also known as contact between meshing gears directly influences productivity as well as durability of a gear assembly [3-7]. In this paper, a comparative analysis of hysteresis stress, strain, and penetration behaviour in three identified spur gear assemblies' designs has been presented [8]. The analysis was aimed to identify the potential causes of the differences in performance among the designs and computation of the recommendations for enhanced efficiency and reliability of spur gear systems [9]. Investigation of the mechanical systems and the systems including gears in particular has critical importance in multiple engineering field. The mechanical systems become more and more fast and get heavier in various applications starting from the automotive sector and ending with the aerospace industry. Therefore, there is a need for gear drives with maximum potential of load-carrying capacity for machinery and equipment [10-13].

Strategies for advancing the load bear capacity of gear drives include improving gear modules and widening gears sizes. Problem is that both these techniques have some drawbacks such as size and the compromise of the potential power-to-weight ratio [14-18]. While most design adjustments can progress the stress condition of gear teeth to some extent, the consequences of design alteration on expanding contact ratio of in-volute gear sets is restricted under ordinary conditions, and it is not appropriate to further increase capacity to bear load [19-23]. The method that is most effective to extend the capacity to bear load is increasing the contact ratio by modifying non-standard gears [24-26]. Overall, the study finds that the differences in design manifest in lower hysteresis losses and more favourable stress and strain distributions in several designs, increasing the efficiency and lifespan of the gear [27-28].

At the same time, higher penetration and stress concentrations visible in several other designs may lead to a significantly higher rate of gear wear and potential premature failure. As such, the study may help to guide the selection of appropriate gear types and materials to achieve optimal mechanical performance [29-32]. The analysis of gear systems is essential for many branches of engineering, as these systems influence how a wide range of other mechanical elements behave. As technological development in the automotive and aerospace sector the demand of reliable gear systems is increasing [33]. Therefore, the continuous pace of innovation in gear design are necessary to meet the exact requirements of the advanced technology [34].

2 CAD Modelling

The flowchart outlines in Fig. 1 the procedure for designing a gear the usage of a CAD device, specially SolidWorks, facilitated by using a graphical user interface (GUI). The manner starts by way of gathering necessary design inputs via the GUI. If enough records isn't to be had, the method loops lower back to collect extra information. Once good enough information is collected, the module calculates primarily based on the loading situations and wellknown empirical family members to determine the most calculated fee of the module. Following this, important geometrical dimensions of the spur gear are calculated the usage of the derived module and empirical standards. These consequences are then displayed at the GUI. In the very last step, the layout gadget mechanically generates the CAD model in Solid Works the usage of macro code, completing the design manner. This systematic technique guarantees

that the equipment is designed successfully and as it should be in keeping with exact necessities.

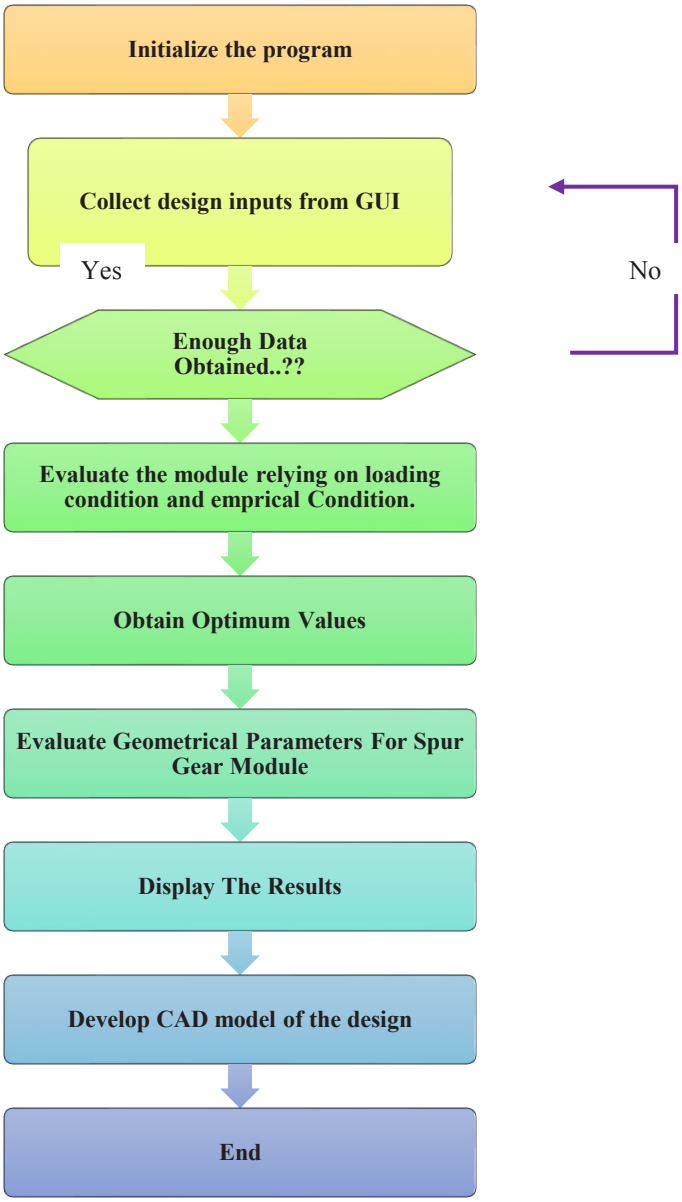

Fig. 1: Process flowchart for the CAD System

3. Methodology

Theoretical analysis:- Neuber's rule equalizes the elastic material behavior strain energy with the real total strain energy near notch point.
Neuber's rule is used to calculate the uniaxial stress state as shown in Fig. 2.

$$\sigma_b . \varepsilon_b = \frac{(K_t . \sigma_{nominal})^2}{E} \quad (1)$$

Where

σ_b = Actual bending stress

ε_b = Actual bending strain

K_t = theoretical stress concentration factor

$\sigma_{nominal}$ = Nominal stress

E = young modulus or modulus of elasticity

$$K_t . \sigma_{nominal} = \sigma_{b,elastic} \quad (2)$$

$\sigma_{b,elastic}$ = bending stress for linear elastic material behavior

$$\sigma_b . \varepsilon_b = \frac{(\sigma_{b,elastic})^2}{E} \quad (3)$$

By considering surface finish factorK_{sf}above equation can be written as

$$\sigma_b . \varepsilon_b = \frac{(\sigma_{b,elastic} . K_{sf})^2}{E} \quad (4)$$

K sf is affected by ultimate tensile strength and surface roughness.

Neuber's rule can also be used to find stable cyclic stress-strain curves using elastic-plastic correction (Ramberg-Osgood curve)

$$\varepsilon_{b,max} = \frac{\sigma_{b,max}}{E} + \left(\frac{\sigma_{b,max}}{K\prime}\right)^{1/n'} \quad (5)$$

Where

$\varepsilon_{b,max}$= maximal actual bending strain

$\sigma_{b,max}$ = maximal actual bending stress

K' = cyclic strength coefficient

n' = cyclic strength exponent

Maximum linear-elastic and actual bending stress and strains

$$\sigma_{b,max} . \varepsilon_{b,max} = \frac{(\sigma_{b,elastic} . K_{sf})^2}{E} \quad (6)$$

$$\frac{(\sigma_{b,elastic} . K_{sf})^2}{E . \sigma_{b,max}} = \frac{\sigma_{b,max}}{E} + \left(\frac{\sigma_{b,max}}{K\prime}\right)^{1/n'} \quad (7)$$

Once the $\sigma_{b,max}$ is found the value of $\varepsilon_{b,max}$ can be obtained, in the above equationK_{sf}, E, K' and n' are established material attributes and $\sigma_{b,max}$ is taken from the FEA analsysi.

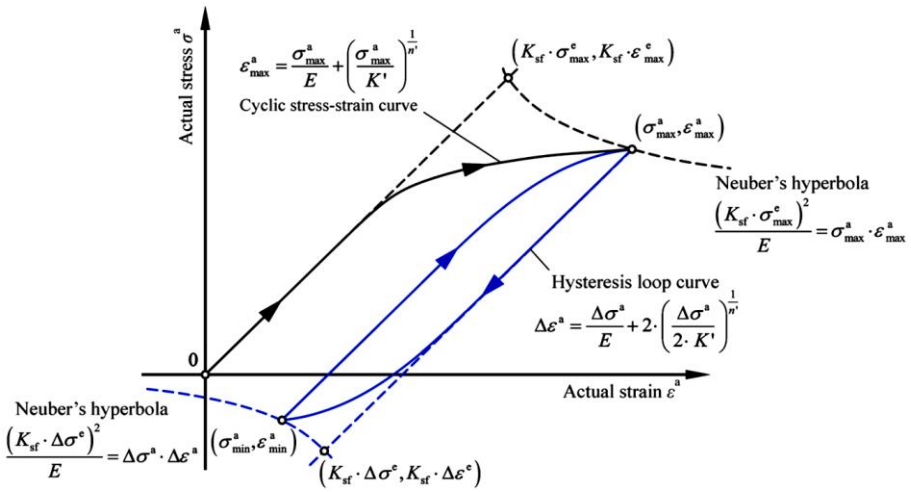

Fig. 2: Neuber's Rule Visualization for Constant Amplitude Cyclic Loading [2]

Hysteresis loop curve can be expressed as

$$\Delta\varepsilon_b = \frac{\Delta\sigma_b}{E} + 2.\left(\frac{\Delta\sigma_b}{2.K\prime}\right)^{1/n\prime} \quad (8)$$

Where

$\Delta\varepsilon_b$ = actual bending strain range

$\Delta\sigma_b$ = actual bending stress range

Optimal Actual Cyclic Bending Stress and Strain can be achieved by

$\sigma_{b,min} = \sigma_{b,max} - \Delta\sigma_b$

$\varepsilon_{b,min} = \varepsilon_{b,max} - \Delta\varepsilon_b$

Actual bending stresses and strains are calculated from linearelastic ones using Neuber's rule and the elastic-plastic correction.

Driving Gear Design Parameters for Design 1-: Here we discuss the geometrical parameters of the driving gear in design 1, the number of teeth are 28 which dictates the meshing properties and the size of gear. The gear module is 3.175 mm it influences tooth dimensions and load bear capacity. Face width determines transmission capability which is 6.35 mm with the pressure angle of 20 degrees. The tip relief of 0.013 mm and root fillet radius of the basic rack enhance durability by reducing stress. The addendum and dedendum of 3.334 mm and 4.286 mm respectively while tip diameter is 95.25 mm which affects size and gear meshing.

Calculation of module from outside diameter of gears (design 2)-: Initially, the outside diameter of gear is derived using $D_o = (n+2)m$ where**,** D_o represents the outer diameter of the driving gear, n signifies the number of teeth = 28, and m denotes the gear module = 3.175 mm and similarly, for $D_1 = (n+2)m$ where D_1 represents the outer diameter of the driven gear, n signifies the number of teeth = 28, and m denotes the gear module = 3.175 mm. This determines the size of gear teeth and efficient power transmission. After this, pitch circle diameter (d) is calculated d = n×m = 88.9 mm. The center distance x = 88.9 mm is determined as the average of the pitch circle diameters, it is essential for maintaining proper gear engagement. At last, the circular pitch p = 9.975 mm is calculated using the formula p=π×m, showing the pitch circle's distance between two adjacent teeth.

4 Results and Discussion

In this research work, the prime intentions of changing the face width of the spur gear Nab will be to improve and enhance the fatigue-life and reduce “contact-pressure” between the teeth of the spur gear assembly through mathematical and finite element analysis. Creo-3 CATIA modeling software has been used for developing three different models of the driving gear. The Catia drawing is then exported to an stp. File. “Design-1” is designed with the dimensional parameter values given in the base paper. Mathematically derived parameter values are followed for the second design, whereas for the third design, the geometrical parameters have been increased by 20% with respect to the base model with the gear module. Steady-state structural analysis, fatigue analysis, and contact analysis are carried out for each gear design. Results of these analyses in this section, detailed discussions of the results of these analyses have been made, and several FEM generated contours and graphs have been depicted under Table 1.

Table 1: Comparative results of Safety Factors for different design of spur gear assembly in different torque

Torque [N_m]	Hysteresis Stress [MPa]	Hysteresis Strain [mm/mm]	Hysteresis Stress [MPa]	Hysteresis Strain [mm/mm]	Hysteresis Stress [MPa]	Hysteresis Strain [mm/mm]
	Design 1		Design 2		Design 3	
350	388.81	0.0116	413.17	0.0145	373.91	0.0097
400	409.04	0.0128	433.91	0.0184	391.69	0.0118
450	427.13	0.0171	452.90	0.0222	407.74	0.0143
500	443.52	0.0198	470.18	0.0263	422.67	0.0169
550	458.74	0.0230	486.45	0.0301	436.53	0.0188
600	472.92	0.0274	501.65	0.0356	449.54	0.0216

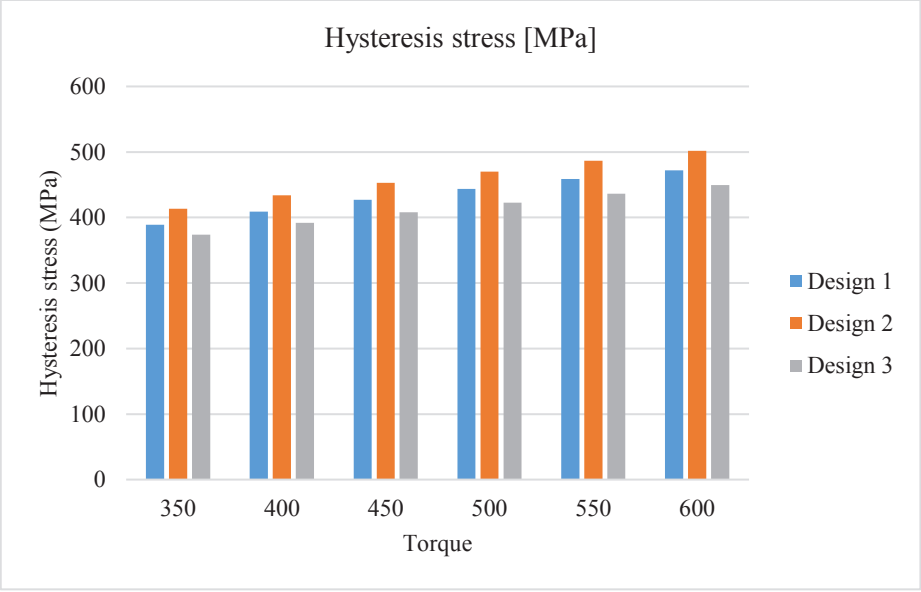

Fig. 3: All designs of spur gear assemblies have been compared for hysteresis stress

As shown in Table 1, the "local elastic-plastic" response at the critical location of the spur gear assembly varies due to the applied torques of 388.81 MPa, 409.04 MPa, 427.13 MPa, 443.52 MPa, 458.74 MPa, 472.92 MPa stress and 0.0116 mm/mm, 0.0128 mm/mm, 0.0171 mm/mm, 0.0198 mm/mm. For design-2 the values are 413.17 MPa, 433.91 MPa, 452.90 MPa, 470.18 MPa, 486.45 MPa, 501.65 MPa stress and 0.0145 mm/mm, 0.0184 mm/mm, 0.0222 mm/mm, 0.0263 mm/mm, 0.0301 mm/mm, 0.0356 mm/mm strain respectively for contact analysis ranges from 350 N-m to 600 N-m. For design-3 the values are 373.91 MPa, 391.69 MPa, 407.74 MPa, 422.67 MPa, 436.53 MPa, 449.54 MPa stress and 0.0097 mm/mm, 0.0118 mm/mm, 0.0143 mm/mm, 0.0169 mm/mm, 0.0188 mm/mm, 0.0216 mm/mm strain respectively for contact analysis ranges from 350 N-m to 600 N-m.

In this figure horizontal parameter shows the torque in N-m and vertical parameters shows Hysteresis stress in MPa of spur gear assembly. The three different bars represent three different designs as shown in Fig. 3. As found in the comparative results, the design-3 spur

gear assembly has a lessened Hysteresis stress of 3.83 % and a lessened Hysteresis stress of 4.74% compared to design-1 at 350 N m and 600 N m, respectively, during testing.

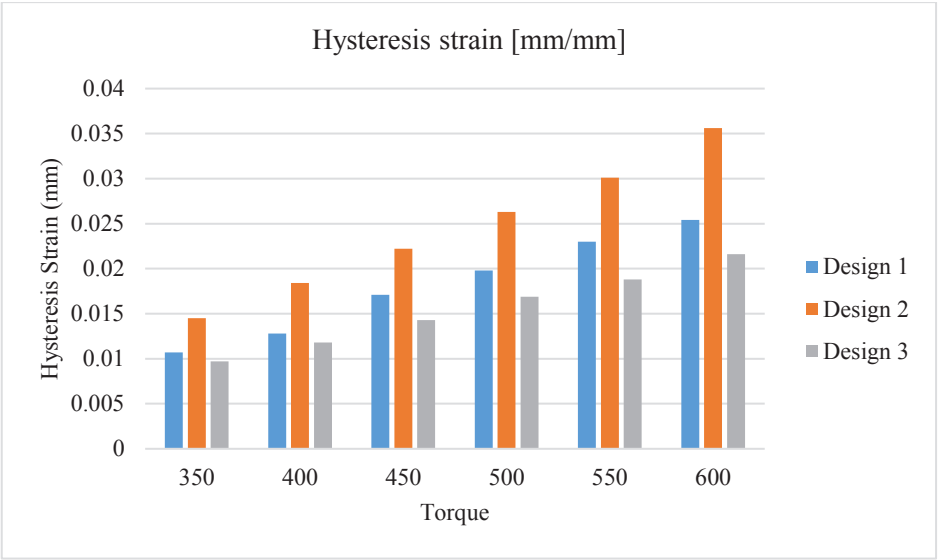

Fig. 4: Comparison of hysteresis strains for different spur gear designs

In this figure horizontal parameter shows the torque in N-m and vertical parameters shows Hysteresis strain in mm/mm of spur gear assembly. The three different bars represent three different designs as shown in Fig. 4. In comparison to design-1, design-3 has a lower Hysteresis strain of 16.37 % at 350 N m and 21.16 % at 600 N m as well as a lower Hysteresis stress at 350 N m, based on comparisons of the Hysteresis stress of spur gear assemblies.

Table 2: Comparative results of Penetration for three different design of spur gear assembly in different torque

Torque [N_m]	**Penetration [mm] Design 1**	**Penetration [mm] Design 2**	**Penetration [mm] Design 3**
350	0.0181	0.02104	0.0186
400	0.0211	0.02381	0.0217
450	0.0238	0.02660	0.0239
500	0.0268	0.02933	0.0267
550	0.0287	0.03209	0.0289
600	0.0320	0.03488	0.0317

According to the results of a finite element analysis performed on spur gear of design-1, the maximum penetration between the contact teeth was 0.0181 mm, 0.0211 mm, 0.0238 mm, 0.0268 mm, 0.0287 mm, and 0.0320 mm. At 350 to 600 Newton-meter, the values for design-2 are 0.02104 mm, 0.02381 mm, 0.02661 mm, 0.02933 mm, 0.03209 mm, and 0.03488 mm at 350 to 600 Newton-meter, respectively. Based on the 350 to 600 Newton-meter range, the values for design-3 are 0.0186 mm, 0.0217 mm, 0.0239 mm, 0.0267 mm, 0.0289 mm, and 0.0317 mm, respectively.

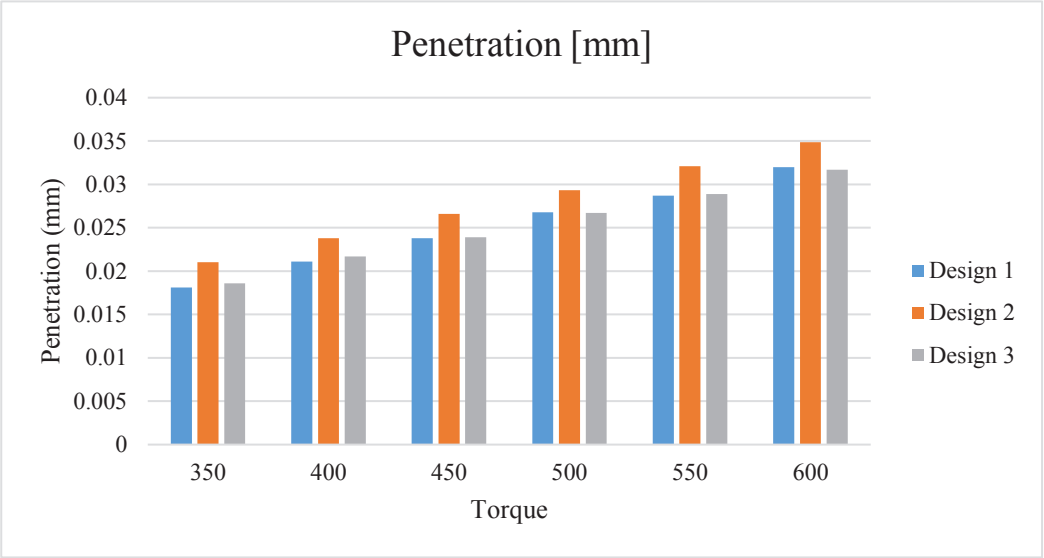

Fig. 5: All designs of spur gear assemblies were compared for penetration results

In this figure 5 horizontal parameter shows the torque in N-m and vertical parameters shows Penetration in mm of spur gear assembly. The three different bars represent three different designs as shown in Fig. 5. There is a slight difference between design-3 and design-1 in terms of penetration at 350 N m and marginally lower penetration at 600 N m compared with design-3 in terms of Hysteresis stress of spur gear assembly. This was confirmed by the comparative results of the Hysteresis test of spur gear assembly.

5 Conclusion

The study conducted on hysteresis stress, strain and penetration for three designs of spur gear assemblies at different torque levels reveals significant information like elastic-plastic responses and structural integrity behavior under different conditions.

Safety Factor:

- In terms of improvement in the safety factor, Design 3 stands out. Its stress and strain values are the lowest compared to those of Designs 1 and 2 throughout the application of torque from a minimum value of 350 N-m to a maximum value of 600 N-m. This design with 20% increase in its geometrical parameters over the base design demonstrates an enhanced capacity to withstand stress with alteration of 4.74% stress reduction at 600 N-m compared to Design 1. The lower strain figure identifies a 21.16% drop at 600 N-m compared to Design 1, further confirming enhancement in its structural integrity and resistance to deformation under load.

Contact Pressure:

- Design 3 has also performed well on the aspect of reducing the contact pressure between the gear teeth. This is still a critical consideration in wear reduction or limitation of wear and determinant for gear operation life. It exhibited the least rise in penetration with the increase in torque, reaching only 0.0317 mm at 600 N-m, which is slightly less than that with Design 1. Such lesser depth of penetration is an indicator of better load distribution across the gear teeth and, hence, less intense localized stress leading to a much safer and more durable gear assembly.

In general we can say that, a comparative analysis emphasizes the importance of hysteresis stress, strain and penetration while designing spur gears. This implies the importance of

design optimization in reducing hysteresis related issues and improves the reliability of spur gear assemblies.

References

1. Bomidi, John AR, and Farshid Sadeghi. "Three-dimensional finite element elastic–plastic model for subsurface initiated spalling in rolling contacts." Journal of Tribology 136, 1 (2014): 011402.
2. Feng, Ke, J. C. Ji, Qing Ni, and Michael Beer. "A review of vibration-based gear wear monitoring and prediction techniques." Mechanical Systems and Signal Processing 182 (2023): 109605.
3. Vivet, Mathijs, Tommaso Tamarozzi, Wim Desmet, and Domenico Mundo. "On the modelling of gear alignment errors in the tooth contact analysis of spiral bevel gears." Mechanism and Machine theory 155 (2021): 104065.
4. Ansari, Irfan Ahmad, Kamal K. Kar, and J. Ramkumar. "Effect of ground tire rubber media's viscoelasticity and flow passage geometry on the abrasive flow finishing of helical gear." Journal of Manufacturing Processes 101 (2023): 219-233.
5. Maputi, Edmund S., and Rajesh Arora. "Multi-objective spur gear design using teaching learning-based optimization and decision-making techniques." Cogent Engineering 6, 1 (2019): 1665396.
6. Ghori, Syed Waheedullah, Ramengmawii Siakeng, Masrat Rasheed, Naheed Saba, and Mohammad Jawaid. "The role of advanced polymer materials in aerospace." In Sustainable composites for aerospace applications, 19-34. Woodhead Publishing, 2018.
7. Liu, Heli, Huaiju Liu, Caichao Zhu, and Robert G. Parker. "Effects of lubrication on gear performance: A review." Mechanism and Machine Theory 145 (2020): 103701.
8. Wang, Yanzhong, Peng Liu, and Delong Dou. "Investigation of load capacity of high-contact-ratio internal spur gear drive with arc path of contact." Applied Sciences 12, 7 (2022): 3345.
9. Tobie, Thomas, Frank Hippenstiel, and Hardy Mohrbacher. "Optimizing gear performance by alloy modification of carburizing steels." Metals 7, 10 (2017): 415.
10. Miler, Daniel, and Matija Hoić. "Optimisation of cylindrical gear pairs: A review." Mechanism and Machine Theory 156 (2021): 104156.
11. Chauhan, Vikash. "A review on effect of some important parameters on the bending strength and surface durability of gears." Int J Sci Res Publ 6, 3 (2016): 289-298.
12. Hussein, Ahmed W., and Mohammad Q. Abdullah. "A novel design for enhancing the surface durability of the spur gear systems." Proceedings of the Institution of Mechanical Engineers, Part C: Journal of Mechanical Engineering Science 236, 18 (2022): 10143-10160.
13. Rajesh, S., P. Marimuthu, P. Dinesh Babu, and R. Venkatraman. "Balanced bending fatigue life for helical gear drives to enhance the power transmission capacity through novel rack cutters." Engineering Failure Analysis 144 (2023): 106989.
14. Kabirifar, Parham, Jonas Trojer, Miha Brojan, and Jaka Tušek. "From the elastocaloric effect towards an efficient thermodynamic cycle." Journal of Physics: Energy 4, 4 (2022): 044009.
15. Jayabal, Ravikumar, Sekar Subramani, Damodharan Dillikannan, Yuvarajan Devarajan, Lakshmanan Thangavelu, Mukilarasan Nedunchezhiyan, Gopal Kaliyaperumal, and Melvin Victor De Poures. "Multi-objective optimization of performance and emission characteristics of a CRDI diesel engine fueled with sapota methyl ester/diesel blends." Energy 250 (2022): 123709.
16. Swarna, K. S. V., Arangarajan Vinayagam, M. Belsam Jeba Ananth, P. Venkatesh Kumar, Veerapandiyan Veerasamy, and Padmavathi Radhakrishnan. "A KNN based

random subspace ensemble classifier for detection and discrimination of high impedance fault in PV integrated power network." Measurement 187 (2022): 110333.
17. Sridhara, V., B. S. Gowrishankar, Snehalatha, and L. N. Satapathy. "Nanofluids—a new promising fluid for cooling." Transactions of the Indian Ceramic Society 68, 1 (2009): 1-17.
18. Alkorbi, Ali S., K. Yogesh Kumar, M. K. Prashanth, L. Parashuram, Antonio Abate, Fahad A. Alharti, Byong-Hun Jeon, and M. S. Raghu. "Samarium vanadate affixed sulfur self-doped g-C3N4 heterojunction; photocatalytic, photoelectrocatalytic hydrogen evolution and dye degradation." International Journal of Hydrogen Energy 47, 26 (2022): 12988-13003.
19. Kumar, CB Pradeep, M. S. Raghu, B. S. Prathibha, M. K. Prashanth, G. Kanthimathi, K. Yogesh Kumar, L. Parashuram, and Fahad A. Alharthi. "Discovery of a novel series of substituted quinolines acting as anticancer agents and selective EGFR blocker: Molecular docking study." Bioorganic & Medicinal Chemistry Letters 44 (2021): 128118.
20. Manohar, T., S. C. Prashantha, H. P. Nagaswarupa, Ramachandra Naik, H. Nagabhushana, K. S. Anantharaju, KR Vishnu Mahesh, and H. B. Premkumar. "White light emitting lanthanum aluminate nanophosphor: near ultra violet excited photoluminescence and photometric characteristics." Journal of Luminescence 190 (2017): 279-288.
21. Srinivasan, K., K. Porkumaran, and G. Sainarayanan. "Improved background subtraction techniques for security in video applications." In 2009 3rd International Conference on Anti-counterfeiting, Security, and Identification in Communication, pp. 114-117. IEEE, 2009.
22. Ram, J. Prasanth, Dhanup S. Pillai, Amer MYM Ghias, and N. Rajasekar. "Performance enhancement of solar PV systems applying P&O assisted Flower Pollination Algorithm (FPA)." Solar Energy 199 (2020): 214-229.
23. Yogananda, H. S., R. B. Basavaraj, G. P. Darshan, B. Daruka Prasad, Ramachandra Naik, S. C. Sharma, and H. Nagabhushana. "New design of highly sensitive and selective MoO3: Eu3+ micro-rods: Probing of latent fingerprints visualization and anti-counterfeiting applications." Journal of colloid and interface science 528 (2018): 443-456.
24. Prakash, Shanmugam, Govindharaj Somiya, Nagaraj Elavarasan, Kasivisvanathan Subashini, Selvaraj Kanaga, Ramamurthy Dhandapani, Magudeeswaran Sivanandam, Poomani Kumaradhas, Chinnasamy Thirunavukkarasu, and Venugopal Sujatha. "Synthesis and characterization of novel bioactive azo compounds fused with benzothiazole and their versatile biological applications." Journal of Molecular Structure 1224 (2021): 129016.
25. SudhirSastry, Y. B., Pattabhi R. Budarapu, N. Madhavi, and Y. Krishna. "Buckling analysis of thin wall stiffened composite panels." Computational Materials Science 96 (2015): 459-471.
26. Sastry, YB Sudhir, Pattabhi R. Budarapu, Y. Krishna, and S. Devaraj. "Studies on ballistic impact of the composite panels." Theoretical and Applied Fracture Mechanics 72 (2014): 2-12.
27. Jayanthi, Neelampalli, B. Vijaya Babu, and N. Sambasiva Rao. "Survey on clinical prediction models for diabetes prediction." Journal of Big Data 4 (2017): 1-15.
28. Ramu, Gandikota. "A secure cloud framework to share EHRs using modified CP-ABE and the attribute bloom filter." Education and Information Technologies 23, 5 (2018): 2213-2233.
29. Lakshmi, L., M. Purushotham Reddy, Chukka Santhaiah, and U. Janardhan Reddy. "Smart phishing detection in web pages using supervised deep learning classification

and optimization technique ADAM." Wireless Personal Communications 118, 4 (2021): 3549-3564.

30. Cheruvu, Aravind, V. Radhakrishna, and N. Rajasekhar. "Using normal distribution to retrieve temporal associations by Euclidean distance." In 2017 International Conference on Engineering & MIS (ICEMIS), pp. 1-3. IEEE, 2017.
31. Vallabhuni, Rajeev Ratna, S. Lakshmanachari, G. Avanthi, and Vallabhuni Vijay. "Smart cart shopping system with an RFID interface for human assistance." In 2020 3rd International Conference on Intelligent Sustainable Systems (ICISS), pp. 165-169. IEEE, 2020.
32. Kumar, K. Udaya, P. Babu, Ch Basavapoornima, R. Praveena, D. Shobha Rani, and C. K. Jayasankar. "Spectroscopic properties of Nd3+-doped boro-bismuth glasses for laser applications." Physica B: Condensed Matter 646 (2022): 414327.
33. Rani, Bandi Mary Sowbhagya, Vasumathi Devi Majety, Chandra Shaker Pittala, Vallabhuni Vijay, Kanumalli Satya Sandeep, and Siripuri Kiran. "Road Identification Through Efficient Edge Segmentation Based on Morphological Operations." Traitement du Signal 38, 5 (2021).
34. Radhakrishna, Vangipuram, P. V. Kumar, V. Janaki, and N. Rajasekhar. "Estimating prevalence bounds of temporal association patterns to discover temporally similar patterns." In International Conference on Soft Computing-MENDEL, 209-220. Cham: Springer International Publishing, 2016